Article

Biomechanical Evaluation of the Lumbar Spine by Using a New Interspinous Process Device: A Finite Element Analysis

Hung-Wen Wei [†], Shao-Ming Chuang [†] and Chen-Sheng Chen *

Department of Physical Therapy and Assistive Technology, National Yang Ming Chiao Tung University, Taipei 112, Taiwan; hungwwei@gmail.com (H.-W.W.); e6978tw@gmail.com (S.-M.C.)
* Correspondence: cschen0623@nycu.edu.tw; Tel.: +886-2-2826-7353
† The authors have the same contribution.

Abstract: Minimally invasive decompression is generally employed for treating lumbar spinal stenosis; however, it results in weakened spinal stability. To augment spinal stability, a new interspinous process device (NIPD) was developed in this study. The biomechanical features of the NIPD were evaluated in this study. Three finite-element (FE) models of the entire lumbar spine were implemented to perform biomechanical analysis: the intact, defect (DEF), and NIPD models. The DEF model was considered for lumbar spines with bilateral laminotomies and partial discectomy at L3–L4. Range of motion (ROM), disc stress, and facet joint contact force were evaluated in flexion, extension, torsion, and lateral bending in the three FE models. The results indicated that ROM in the extension increased by 23% in the DEF model but decreased by 23% in the NIPD model. In the NIPD model, the cephalic adjacent disc stress in flexion and extension was within 5%, and negligible changes were noted in the facet joint contact force for torsion and lateral bending. Thus, the NIPD offers superior spinal stability and causes only a minor change in cephalic adjacent disc stress in flexion and extension during the bilateral laminotomy and partial discectomy of the lumbar spine. However, the NIPD has a minor influence on the ROM and facet joint force for lateral bending and torsion.

Keywords: interspinous process device; lumbar spine; finite-element model; biomechanics

1. Introduction

Lumbar spines have a three-point joint, including a facet joint and spinal disc. Spinal stenosis in the lumbar spine is caused by a hypertrophic facet joint or bulged disc. The hypertrophic ligamentum flavum may also impinge the spinal cord and induce spinal stenosis. The aforementioned scenarios can result in nerve root or spinal cord compression [1]. Decompression laminectomy is employed to open the spinal canal and decompress the spinal cord [2]. Approaches for removing lamina for decompression include partial or total laminectomy. In clinical settings, laminectomy sometimes results in iatrogenic spondylolisthesis because the surgery involves the removal of excessive posterior elements and the cutting of posterior spinal ligaments, which induce spinal instability [3,4]. In decompression surgery, the spinal ligament must be retained as much as possible to maintain spinal stability. Laminectomy helps preserve the interspinous and supraspinous ligaments and thus assists in stabilizing spinal motion in flexion [5]. Therefore, partial removal of the lamina, such as in laminotomy, not only decompresses the spinal cord but also allows for the achievement of spinal stability.

In addition to the risk of spinal surgery in laminotomy, appropriate reconstruction is critical for strengthening spinal stability. In clinics, many interspinous process devices, such as the DIAM and Coflex, are used to enhance spinal stability and prevent the narrowing of the foramen in extension. In addition, interspinous process devices can effectively reduce the load on facet joints and enable some movement on the motion segment [6]. Compared with rigid devices, such as spinal fixators, interspinous process devices offer enhanced spinal stability. The interspinous process device Coflex exhibited advantages in stabilizing

the surgical level, especially in flexion and extension, but it was too rigid and increased facet joint contact force at the adjacent level by 27% [7]. Additionally, it also caused spinal process fracture in clinical application [8]. The interspinous process DIAMs are made of silicone rubber and provide impact absorption between the interspinous processes in extension. Since the DIAM is not made of metal, its stiffness is less than that of Coflex, which is made of metal. DIAMs lower the risk of spinal process fractures. Therefore, they are used to treat lumbar spine disorders related to neuropathology [9,10]. However, DIAMs are not as rigid as the traditional metal spinal fixator. Additionally, the DIAM is a V-shape design and offers less stability in torsion [11]. Therefore, a new interspinous process device (NIPD) was developed in this study.

The design and efficacy of new orthopaedic implants can be evaluated through in vitro or in vivo experiments. However, the results of these experiments differ according to differences in cadaveric specimens. Finite element (FE) methods are widely used to evaluate the biomechanical behavior of implants [12–15]. Chen and Shih implemented an FE method with topology optimization to design an interspinous process device [12]. They removed redundant material to redesign the device and evaluated its biomechanical characteristics. This study demonstrated that the new device provided more stability at the instrumented level than the DIAM system, especially in lateral rotation and bending direction. Bae et al. also conducted an FE model of the five-level lumbar spine to analyze the biomechanics of a new interspinous device [15]. They demonstrated that the spinal cage combined with a new interspinous device could reduce range of motion (ROM) of the lumbar spine at least 40% in flexion, extension, torsion, and lateral bending.

Many studies have employed FE methods to design or evaluate interspinous process devices, such as soft DIAMs or rigid Coflex. Therefore, this study created a U-shape interspinous process device. Compared to DIAMs, it provides more contact area around the interspinous process to increase spinal stability. This study expected that a new U-shape device could reach the goal of resisting extension moment. Therefore, the objective of this study is to evaluate the biomechanical characteristics of the developed NIPD. Biomechanical parameters, such as ROM, disc stress and facet joint force, were evaluated in the study.

2. Materials and Methods

2.1. FE Model of the Intact Lumbar Spine

An FE model of the lumbar spine has been created in previous studies by using FE software (ANSYS 14.0, ANSYS Inc., Canonsburg, PA, USA) [5,11,12,16], as shown in Figure 1. Computer-assisted tomographic images of the normal ligamentous lumbar spine of a male subject were obtained using transverse slices at every 3 mm interval. Each CT slice was acquired from the coronal plane and enlarged in order to identify the different regions of the tissues. Furthermore, 43% of the cross-sectional area of the disc was defined as the nucleus, which is within the range of 30–50% reported in a previous study [16]. This FE model consists of L1–L5 vertebrae, intervertebral discs, posterior elements, and seven ligaments. The spinal disc consists of 12 double-cross-linked fiber layers embedded in the ground substance and incompressible nucleus pulposus. The disc ground substance was modeled using an incompressible, hyperelastic, two-parameter (C1 and C2) Mooney–Rivlin formulation. All seven ligaments were simulated using a two-node truss element (LINK 10) with uniaxial tension resistance-only behavior. The facet joint surfaces were treated as having sliding contact behavior by using an eight-node surface-to-surface contact element, and the coefficient of friction was set as 0.1. A more detailed description of the material properties of the spine FE model can be found in our previous studies, as listed in Table 1 [5,6,11,12].
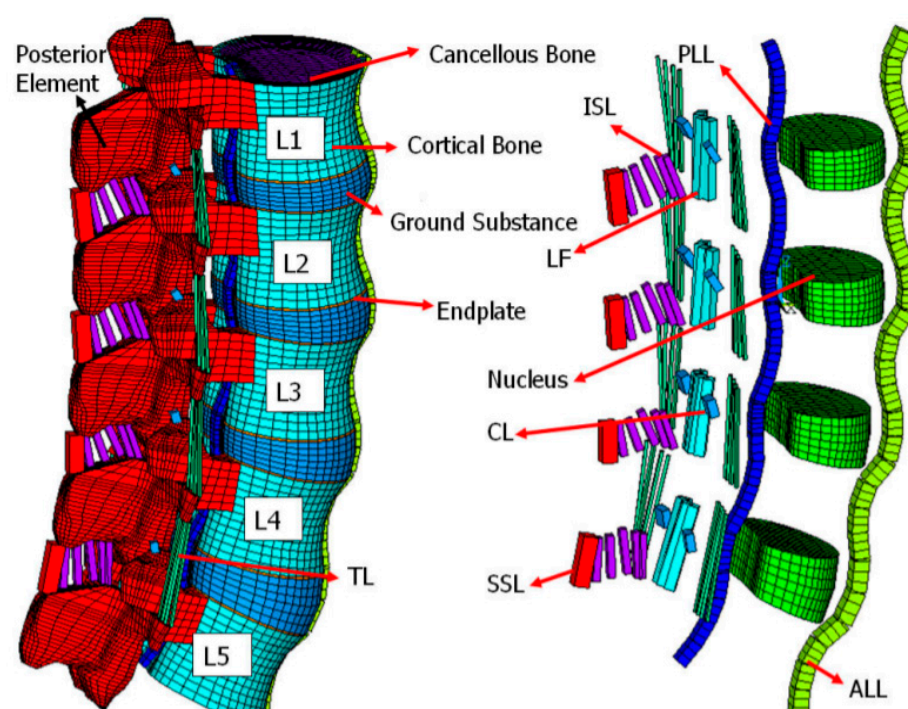
Figure 1. FE model of intact lumbar spine. Note: ALL = anterior longitudinal ligament; CL = capsular ligament; ISL = interspinous ligament; LF = ligamentum flavum; PLL = posterior longitudinal ligament; SSL = supraspinous ligament; TL = transverse ligament.

Table 1. Material properties of lumbar spine.

Material	Element Type	Young's Modulus (MPa)	Poisson's Ratio	Area (mm^2)
Bone				
Cortical	8-node SOLID185	Ex = 11,300	νxy = 0.484	-
		Ey = 11,300	νxz = 0.203	-
		Ez = 22,000	νyz = 0.203	
		Gx = 3800		
		Gy = 5400		
		Gz = 5400		
Cancellous	8-node SOLID185	Ex = 140	νxy = 0.45	-
		Ey = 140	νxz = 0.315	
		Ez = 200	νyz = 0.315	
		Gx = 48.3		
		Gy = 48.3		
		Gz = 48.3		
Posterior element	8-node SOLID185	3500	0.25	-
Disc				
Nucleus pulposus	8-node SOLID185	1.66	0.499	-
Ground Substance	8-node SOLID185	5.36	0.45	-

Table 1. *Cont.*

| Material	Element Type	Young's Modulus (MPa)	Poisson's Ratio	Area (mm^2)
		$C_{10} = 0.42$	$C_{01} = 0.105$	
Annulus Fibers	2-node LINK10			
Outermost		550	-	0.76
Second		495	-	0.5928
Third		412.5	-	0.4712
Innermost		357.5	-	0.3572
Endplate	8-node SOLID185	24	0.4	-
Ligament	2-node LINK10			
ALL		7.8	-	24
PLL		10	-	14.4
TL		10	-	3.6
LF		15	-	40
ISL		10	-	26
SSL		8	-	23
CL		7.5	-	30

C10, C01 indicated two parameters of Mooney–Rivlin hyperelastic formation; d, material incompressibility parameter; ALL, anterior longitudinal ligament; CL, capsular ligament; ISL, interspinous ligament; LF, ligamentum flavum; PLL, posterior longitudinal ligament; SSL, supraspinous ligament; TL, transverse ligament.

To verify the accuracy of the aforementioned FE model, a convergence test was conducted in a previous study [9]. Three mesh densities (coarse model: 4750 elements/4960 nodes; normal model: 27,244 elements/30,630 nodes; finest model: 112,174 elements/94,162 nodes) were selected to study the ROM in the intact lumbar spine (INT) model. The finest mesh density (FE model: 112,174 elements/94,162 nodes) was selected because the differences between the normal model and the finest model were within 1.03% in flexion (less than 0.2°), 4.39% in extension (less than 0.5°), 0.01% in torsion (less than 0.2°), and 0.001% in lateral bending (less than 0.1°) [10]. The element size was approximately 2.5 mm to confirm the accuracy of the FE analysis.

To validate the FE model, the FE analysis results were compared with the results of the in vitro cadaveric tests [16] for the same loading conditions. For model validation [16,17], the ROM in the five levels of the intact model was validated using previous cadaveric in vitro tests. The FE intact model displayed stiffer behavior in flexion, with a ROM value that was 4° less than that described in Rohlmann's in vitro study. In addition, softer results were obtained in torsion compared with the in vitro test data; however, the differences were still within 2°. Overall, the discrepancy between the in vitro tests and our FE simulation was within one standard deviation. The ROMs under four physiological motions fell within similar ranges, and the trends agreed well with the experimental results [17].

2.2. FE Model of a Lumbar Spine with Decompression and the NIPD

To study lumbar spines with decompression, a defect model of the lumbar spine with bilateral laminotomies and partial discectomy at L3–L4 was created in this study, as displayed in Figure 2.
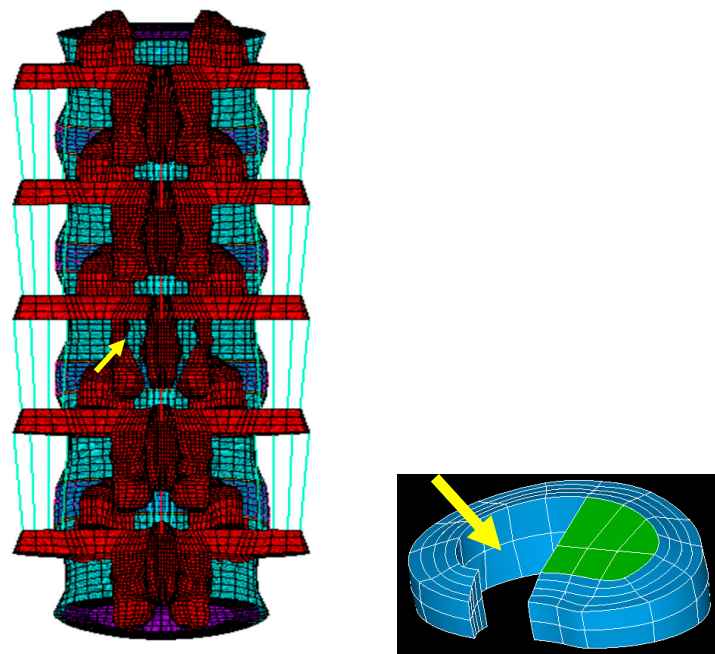
Figure 2. Defect model of the lumbar spine. The L3–L4 disc was partially removed from the ground substance and nucleus. The posterior element at the L3 level was also partially removed. Note: the arrow indicates the location of removed parts.

The designed NIPD is U-shaped and offers high stability because it has a larger contact area than conventional DIAMs, as depicted in Figure 3. The NIPD was implanted in the motion segment of L3–L4. To simulate the surgical procedure, the interspinous ligaments were removed. Since the NIPD is tied to the spinous process by using cables during surgery, bonded contact elements were added between the NIPD and spinous process to ensure that the NIPD did not move. Three FE models were constructed: the INT model (94,162 nodes, 112,174 elements), a lumbar spine model with bilateral laminotomies and partial discectomy at L3–L4 [the defect (DEF) model; 189,824 nodes, 228,538 elements], and a lumbar spine model with bilateral laminotomies and partial discectomy with the NIPD placed at L3–L4 (NIPD model; 199,969 nodes, 296,818 elements).
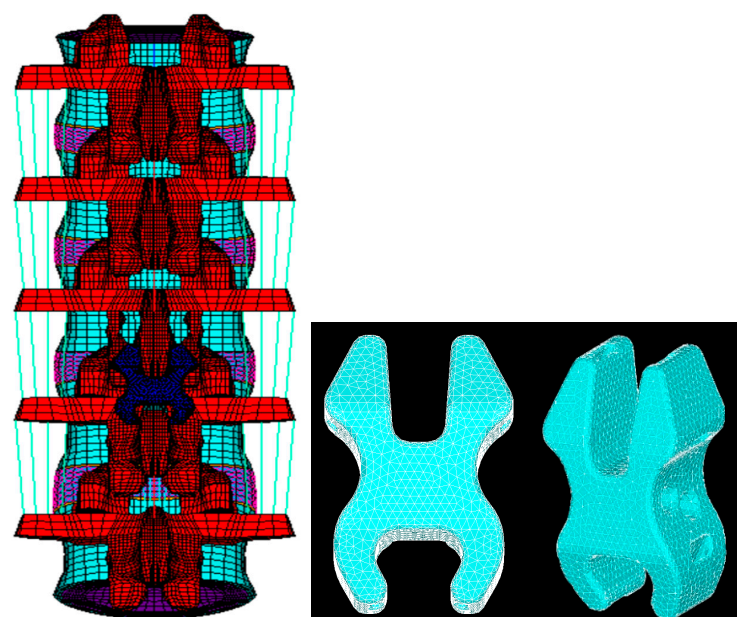

Figure 3. FE model of the lumbar spine with the NIPD.

To study spinal stability, the ROM of the lumbar spine was determined using FE analysis. In general, the lumbar spine with a spinal implant exhibited iatrogenic effects at times, especially in adjacent discs and the facet joint. To investigate the influence of the NIPD on the spinal disc and facet joint, the disc stress and facet joint contact force were analyzed in this study.

2.3. Boundary and Loading Conditions

The bottom of the fifth vertebrae was fixed in the lumbar spine models. Panjabi reported that the hybrid method of displacement control was adequate in evaluating the adjacent level and implanted level in the lumbar spine [18]. Therefore, the FE models were subjected to two load steps. In the first load step, an axial load of 150 N was applied perpendicular to the top of the L1 vertebrae. In the second load step, unconstrained moments were applied to the FE models in flexion (14°), extension (6°), lateral bending (23°), and axial rotation (4°), as shown in Figure 4. These loading conditions were considered in physiological activities and convergence regions of the FE model. Details on the ROM, disc stress, and facet joint were collected in the FE analysis. Since adjacent iatrogenic degeneration is sometimes observed in the cephalic segment, we focused on the ROM and disc stress of the adjacent level L2–L3.
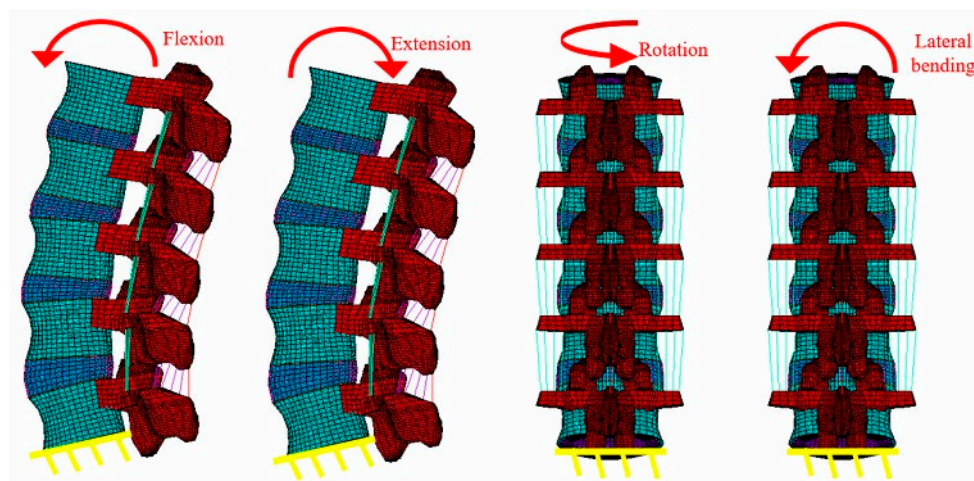
Figure 4. Different loading conditions on the lumbar spine.

3. Results

3.1. Flexion

Compared with the INT model, the DEF and NIPD models exhibited a 10% higher and 18% lower ROM, respectively, for the L3–L4 motion segment (Table 2) during flexion. After implanting the NIPD, the stiffness of the L3–L4 motion segment increased by approximately 37%. In the other motion segments, the differences between all the models were within 8%.

The disc stress distribution at the L3–L4 bridged level in the anterior region was higher in the DEF model than in the NIPD model, as displayed in Figure 5A. In the adjacent level (L2–L3), the stress increase in the NIPD model was within 5% and the stress distribution had no remarkable change on the NIPD model, as depicted in Figure 5B. In addition, no contact force was observed at the facet joint in the three FE models.

3.2. Extension

Compared with the INT model, the DEF and NIPD models exhibited a 23% higher and 23% lower ROM, respectively, for the L3–L4 motion segment during extension. The NIPD increased spinal stability during extension (Table 3).

Table 2. Comparison of the biomechanical characteristics among the three FE models in flexion.

	INT Moment: 4.8 Nm		DEF Moment: 4.5 Nm		NIPD Moment: 5.4 Nm	
ROM (degree)						
L1–L2	3.25		3.11		3.50	
L2–L3	3.30 (100%)		3.13 (95%)		3.45 (105%)	
L3–L4	3.30 (100%)		3.64 (110%)		2.72 (82%)	
L4–L5	4.73		4.71		5.10	
Total	14.58		14.59		14.77	
Stiffness (Nm/degree)						
L3–L4	1.45 (100%)		1.24 (86%)		1.99 (137%)	
Disc max. stress (KPa)						
L2–L3	631 (100%)		604 (96%)		664 (105%)	
L3–L4	535 (100%)		540 (101%)		500 (93%)	
Facet joint force (N)						
	Left	Right	Left	Right	Left	Right
L2–L3	0	0	0	0	0	0
L3–L4	0	0	0	0	0	0

Note: values in parentheses represent the normalized results ([[DEF or NIPD]/INT] × 100%).


(**A**)

(**B**)
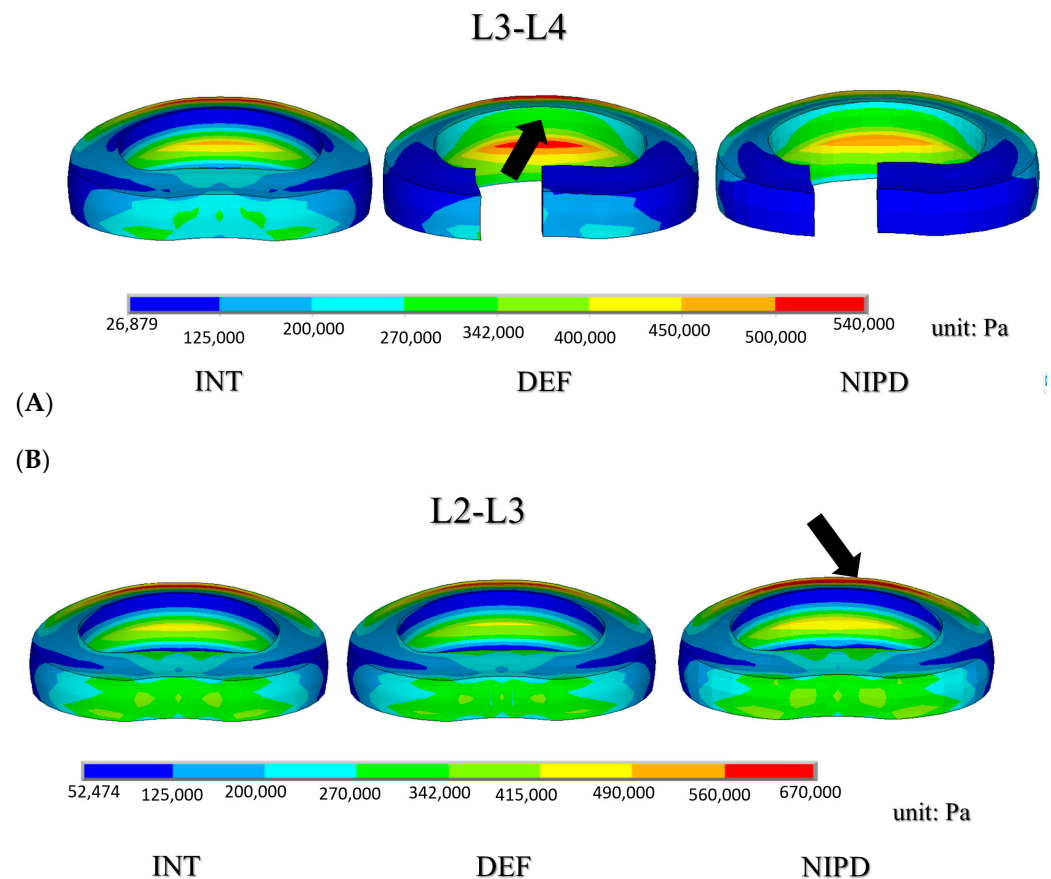
Figure 5. Disc stress distributions in the three FE models during flexion: (**A**) implanted level L3–L4 and (**B**) adjacent level L2–L3. Note: the arrow indicates the region of high stress.

Table 3. Comparison of the biomechanical characteristics among the three FE models during extension.

	INT Moment: 4.5 Nm		DEF Moment: 4.5 Nm		NIPD Moment: 5.1 Nm	
ROM (degree)						
L1–L2	2.12		2.12		2.29	
L2–L3	1.76 (100%)		1.79 (102%)		1.91 (109%)	
L3–L4	1.37 (100%)		1.69 (123%)		1.05 (77%)	
L4–L5	0.92		0.81		1.27	
Total	6.17		6.41		6.52	
Stiffness (Nm/degree)						
L3–L4	3.28 (100%)		2.67 (81%)		4.85 (148%)	
Disc max. stress (KPa)						
L2–L3	355 (100%)		357 (100%)		356 (100%)	
L3–L4	281 (100%)		505 (179%)		381 (135%)	
Facet joint force (N)						
	Left	Right	Left	Right	Left	Right
L2–L3	26	26	26	26	42	41
L3–L4	36	36	36	35	15	14

Note: values in parentheses represent the normalized results ([[DEF or NIPD]/INT] × 100%).

Compared with the DEF model, the NIPD also guided stress flow into the posterior element and reduced the stress at the anterior vertebral body, as depicted in Figure 6. In the L3–L4 bridged level disc, the stress increased by 80% in the DEF model and focused on the posterior region (Figure 7A). In the adjacent level (L2–L3), the disc stress in the NIPD model was the same as in the INT model (Figure 7B). Moreover, at the L3–L4 bridged level, the facet joint contact force decreased by approximately 58% in the NIPD model compared with the INT and DEF models.
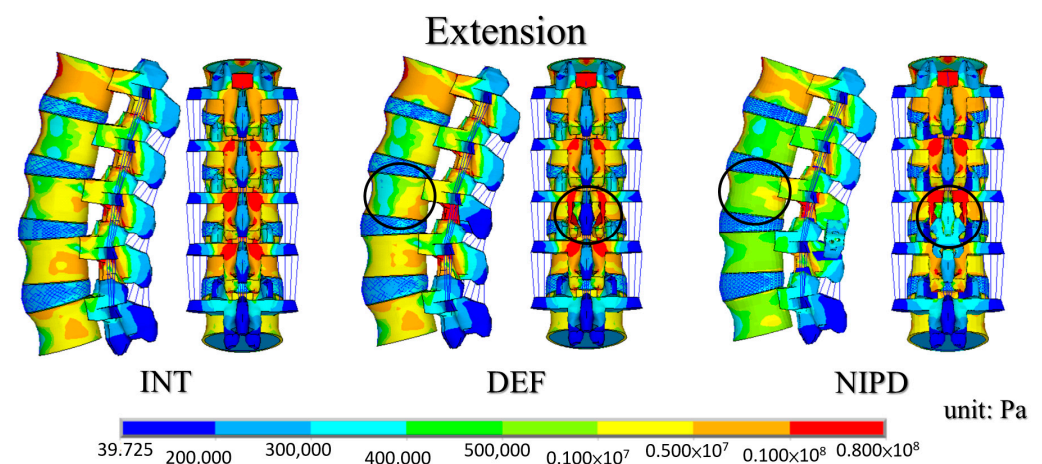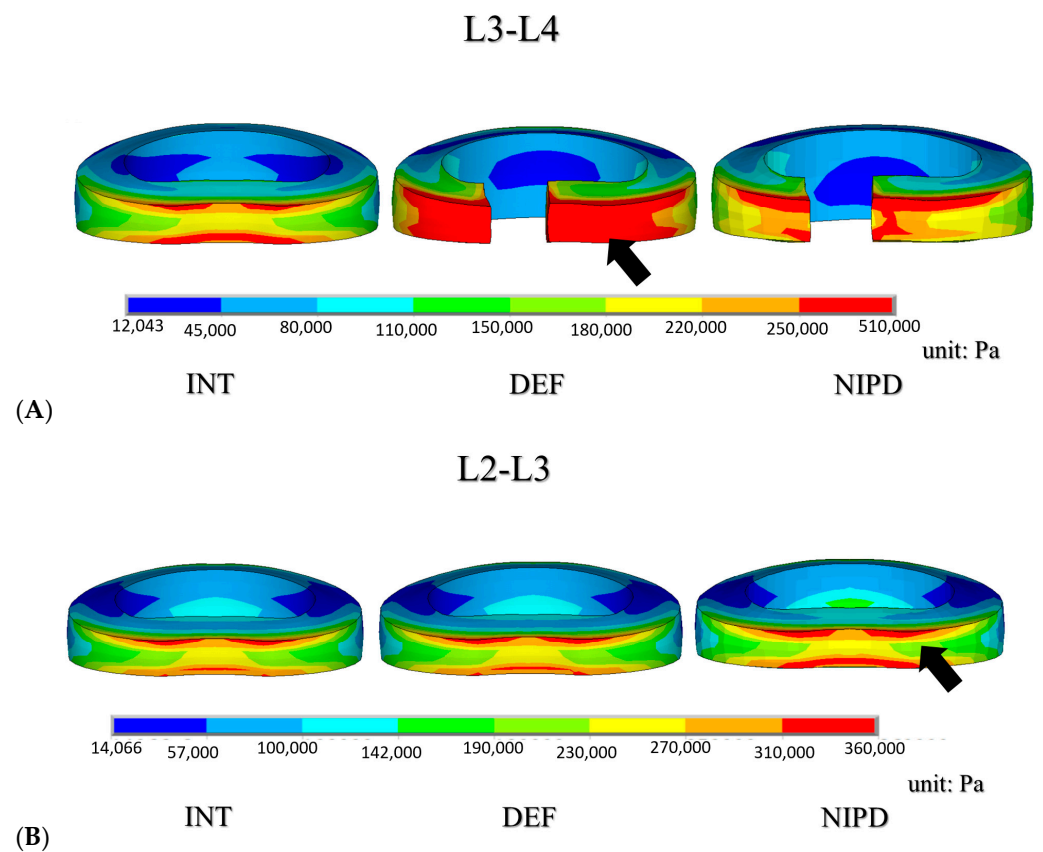

Figure 6. Stress distribution in the lumbar spine in the three FE models. Note: the circle indicates the location of the stress alteration. In the NIPD, the posterior element had higher stress (large area in red color), but the anterior vertebral body had lower stress (small area in yellow color).

3.3. Lateral Bending and Rotation

In lateral bending, the differences between the three FE models in terms of the ROM and stiffness at adjacent level L2–L3 were within 5% (Table 4). In disc stress distributions, these FE models exhibited similar patterns, as displayed in Figure 8. In rotation, the ROM increased by 28% and 16% in the DEF and NIPD models, respectively, compared with the INT model. In the disc stress and facet joint, only minor changes were noted in the FE models (Table 5). Moreover, the change in the facet joint force in rotation and lateral bending was within 5 N in all three models.
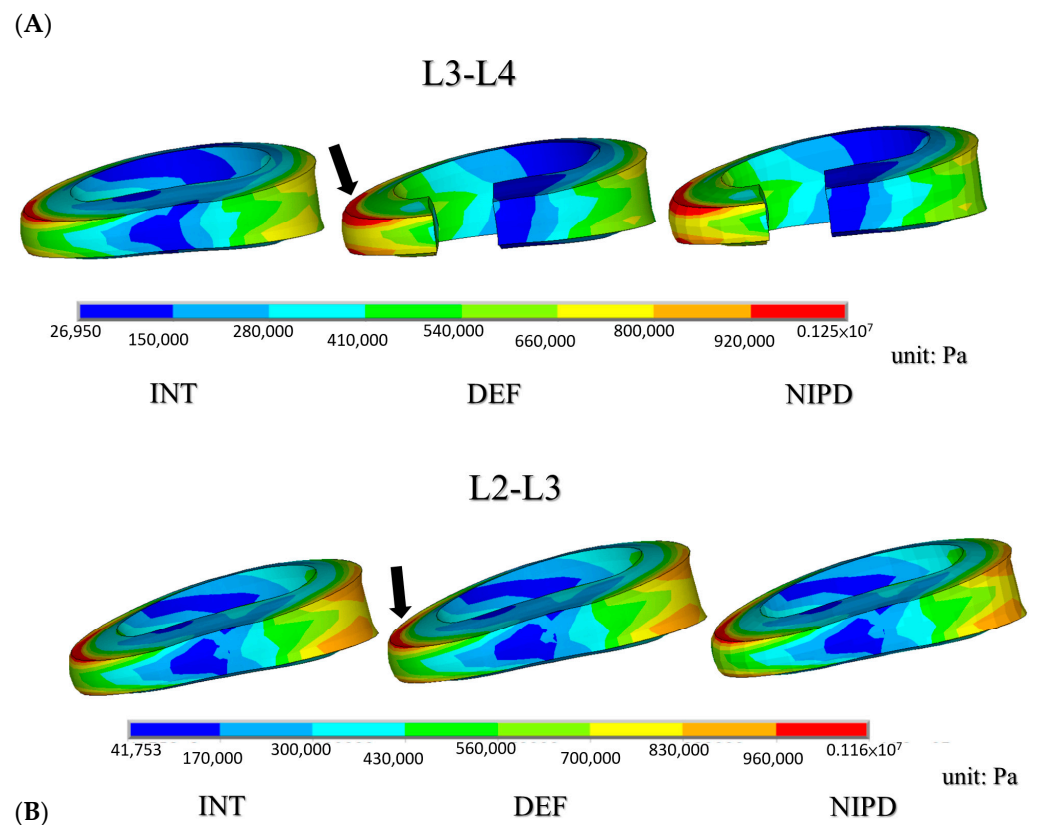
L3-L4

(**A**)

L2-L3

(**B**)

Figure 7. Disc stress distribution in the three FE models in extension: (**A**) implanted level L3–L4 and (**B**) adjacent level L2–L3. Note: the arrow indicates the region of high stress.

Table 4. Comparison of the biomechanical characteristics among the three FE models in lateral bending.

	INT Moment: 12.9 Nm		DEF Moment: 12.6 Nm		NIPD Moment: 12.6 Nm	
ROM (degree)						
L1–L2	6.55		6.41		6.41	
L2–L3	5.89 (100%)		5.75 (98%)		5.76 (98%)	
L3–L4	5.51 (100%)		5.74 (104%)		5.70 (103%)	
L4–L5	5.16		5.19		5.20	
Total	23.11		23.09		23.07	
Stiffness (Nm/degree)						
L3–L4	2.34 (100%)		2.20 (94%)		2.21 (96%)	
Disc max. stress (KPa)						
L2–L3	1110 (100%)		1080 (97%)		1090 (98%)	
L3–L4	1050 (100%)		1240 (118%)		1220 (116%)	
Facet joint force (N)						
	Left	Right	Left	Right	Left	Right
L2–L3	29	20	24	17	24	16
L3–L4	15	3	13	2	18	1

Note: values in parentheses indicate normalized results ([[(DEF or NIPD]/INT] × 100%).

Figure 8. Disc stress distribution in the three FE models in lateral bending: (**A**) implanted level L3–L4 and (**B**) adjacent level L2–L3. Note: the arrow indicates the region of high stress.

Table 5. Comparison of biomechanical characteristics among the three FE models in torsion.

	INT Moment: 1.2 Nm		DEF Moment: 1.2 Nm		NIPD Moment: 1.2 Nm	
ROM (degree)						
L1–L2	0.82		0.82		0.82	
L2–L3	0.82 (100%)		0.82 (100%)		0.82 (100%)	
L3–L4	1.01 (100%)		1.29 (128%)		1.17 (116%)	
L4–L5	1.22		1.23		1.28	
Total	3.87		4.16		4.09	
Stiffness (Nm/degree)						
L3–L4	1.19 (100%)		0.93 (78%)		1.03 (86%)	
Disc max. stress (KPa)						
L2–L3	211 (100%)		210 (100%)		210 (100%)	
L3–L4	271 (100%)		281 (105%)		278 (104%)	
Facet joint force (N)						
	Left	Right	Left	Right	Left	Right
L2–L3	0	15	0	15	0	15
L3–L4	0	13	0	12	0	8

Note: values in parentheses indicate the normalized results ([[DEF or NIPD]/INT] × 100%).

4. Discussion

Traditional laminectomy is a common lumbar decompression surgery and involves the removal of the lamina, ligamentum flavum, supraspinous ligament, and interspinous ligament. However, such spinal decompression can cause iatrogenic spinal instability because the supraspinous and interspinous ligaments help in stabilizing the lumbar spine

in flexion. Moreover, extensive wound areas occur in late recovery. Therefore, minimally invasive laminotomy is an effective treatment because it entails a small wound area and is reported to yield good outcomes [19]. The proposed laminotomy procedure aims to preserve the spinous process, interspinous ligaments, and facet capsules, removing only the bilateral half of the inferior part of the upper lamina and a limited amount of the superior part of the lower lamina, including the adjacent ligamentum flavum, in the treated segment. However, a part of the posterior lamina is destroyed, which decreases the stability of the lumbar spine. The results of this study indicate that the ROM of the laminotomies in the DEF model increased by 16% in flexion, 23% in extension, 4% in lateral bending, and 28% in rotation compared with the corresponding values in the INT model. The results of this study were consistent with those of previous studies that have reported that partial discectomy increases the ROM at the decompressed lumbar segment [20,21]. The increased ROM can induce the impingement of the nerve root and narrow the foramen. Especially in flexion and extension, both motions frequently act on the lumbar spine in daily activities. Therefore, an interspinous process device is essential for augmenting spinal stability after spinal decompression. Consequently, we developed an NIPD. The ROM in the NIPD model was 18% and 23% lower than that in the INT model in flexion and extension, respectively; thus, the NIPD model increased the spinal stability in flexion and extension. We investigated the use of a currently used interspinous process device, namely the DIAM, by using the FE model that was employed in the previous study in which laminotomy with the DIAM was analyzed [11]. This study reported that the DIAM increased the ROM by 10% in flexion and by 17% in extension, as listed in Table 6. Thus, the NIPD outperforms the DIAM. The superior performance of the NIPD can be attributed to its shape. The DIAM is V-shaped, whereas the NIPD is U-shaped; thus, the NIPD provides a larger contact area with the spine than the DIAM and mitigates an excessive increase in ROM. Therefore, the NIPD (−62%) decreased the facet contact force to a greater extent than the DIAM (−29%) at the surgery level in extension. However, the fixation effects of the NIPD and the DIAM in torsion are less suitable than those in extension because when the NIPD and the DIAM are placed at the midline of the lumbar spine, the fixation effect is limited and an asymmetrical load is generated. If the lumbar spine exhibits spinal cord compression and spinal instability, rigid spinal instruments such as rods and screws, rather than the semirigid interspinous process devices discussed in this paper, are required to stabilize the lumbar spine.

Table 6. Comparison between the NIPD and the current device DIAM in the normalized data in the INT model ([DIAM or NIPD]/INT] × 100%).

	Flexion	Extension	Rotation	Lateral Bending
DIAM [11]	110%	117%	109%	116%
NIPD	105%	77%	116%	103%

Studying the variations in the disc stress distribution in the in vitro test was difficult. FE simulation helps in observing the different stresses for different lumbar spine implants. In the validation of disc stress, the disc compressive stress pattern in FE simulation was consistent with the intradiscal pressure pattern in the in vitro test in our previous study [22]. Therefore, we analyzed the disc stress in this study because disc stress is associated with compression of the spinal cord. We found that the disc stress increased in the DEF model at the surgery level in flexion and extension. Laminotomy not only decreased the spinal stability but also increased the disc stress after spinal decompressive surgery. Therefore, laminotomy with the NIPD can help mitigate the increase in disc stress at the bridged level. Swanson et al. [23] found that the implantation of an interspinous process device has limited influence on the adjacent disc; our results also exhibited a similar trend. The NIPD increased the stress at the cephalic adjacent level by less than 5% compared with

the INT model. Thus, the NIPD can help avoid stress-related discogenic back pain at the adjacent level.

In the NIPD model, the facet joint contact force in extension was low and changed negligibly in torsion and lateral bending. The aforementioned results are consistent with those presented by Minns and Walsh, who reported that implantation of an interspinous process device decreases the facet joint stress at the implanted level [24]. Since the NIPD is placed at the central position of the lumbar spine, it successfully resists the extension moment. The placement of the NIPD was similar to that of the DIAM. The decrease in the facet joint contact force achieved using the NIPD (58%) was higher than that achieved using the DIAM (29%) because the U-shaped NIPD provides higher stability than does the V-shaped DIAM in extension [11]. However, the change in torsion and lateral bending was negligible because the NIPD or the DIAM was placed at the central position and the resistance of the asymmetric twisting moment was limited.

This study has some limitations. The FE analysis was similar to the traditional in vitro test in which an experimental load acts on the lumbar spine without muscle. However, in daily activities, the lumbar spine may bear greater physiological loads than the loading conditions tested in the FE model. Especially in the DEF model, activation of the erector spinae muscle would raise extension moment and increase spinal instability. The NIPD may offer more spinal stability because it can effectively resist extension moment. Minimally invasive decompression surgery is typically performed on the elderly population; however, degenerations such as osteophytes, osteoporosis, narrowing foramen, and decreasing disc height were not considered in the developed FE model. In practice, DIAMs are tied to the lumbar spine with cables. Accordingly, contact elements were used in this study to bond the lumbar spine and the NIPD. If the spinal surgeon does not secure the NIPD with the lumbar spine by using cables, the NIPD might become dislodged, and the resulting situations would not match those studied in the FE analysis. Considering the aforementioned limitations, the conclusions of this study are presented in the following text.

5. Conclusions

In this study, an NIPD was developed to enhance the spinal stability for spinal decompression with laminotomies. The NIPD offered increased spinal stability in flexion and extension, and a negligible change in stability was observed in lateral bending. In addition, the NIPD reduced the facet contact force at the bridged level without affecting the cephalic adjacent disc stress in extension. The NIPD also caused a minor change in the facet joint contact force in lateral bending and torsion.

Author Contributions: Conceptualization, H.-W.W.; methodology, S.-M.C.; investigation, S.-M.C.; resources, H.-W.W.; writing—original draft preparation, S.-M.C. and C.-S.C.; writing—review and editing, C.-S.C.; supervision, C.-S.C. All authors have read and agreed to the published version of the manuscript.

Institutional Review Board Statement: Not applicable.

Informed Consent Statement: Not applicable.

Data Availability Statement: The data presented in this study are available on request from the corresponding author.

Conflicts of Interest: The authors declare no conflict of interest.

References

1. Bresnahan, L.; Ogden, A.T.; Natarajan, R.N.; Fessler, R.G. A biomechanical evaluation of graded posterior element removal for treatment of lumbar stenosis: Comparison of a minimally invasive approach with two standard laminectomy techniques. *Spine* **2009**, *34*, 17–23. [CrossRef]
2. Schatzker, J.; Pennal, G.F. Spinal stenosis, a cause of cauda equina compression. *J. Bone Joint Surg. Br.* **1968**, *50*, 606–618. [CrossRef]

3.   Tuite, G.F.; Doran, S.E.; Stern, J.D.; Mc Gillicuddy, J.E.; Papadopoulos, S.M.; Lundquist, C.A.; Oyedijo, D.I.; Grube, S.V.; Gilmer, H.S.; Schork, M.A. Outcome after laminectomy for lumbar spinal stenosis. Part II: Radiographic changes and clinical correlations. *J. Neurosurg.* **1994**, *81*, 707–715. [CrossRef] [PubMed]

4.   Tuite, G.F.; Stern, J.D.; Doran, S.E.; Papadopoulos, S.M.; Mc Gillicuddy, J.E.; Oyedijo, D.I.; Grube, S.V.; Lundquist, C.; Gilmer, H.S.; Schork, M.A. Outcome after laminectomy for lumbar spinal stenosis. Part I: Clinical correlations. *J. Neurosurg.* **1994**, *81*, 699–706. [CrossRef] [PubMed]

5.   Chen, C.S.; Feng, C.K.; Cheng, C.K.; Tzeng, M.J.; Liu, C.L.; Chen, W.J. Biomechanical analysis of the disc adjacent to posterolateral fusion with laminectomy in lumbar spine. *J. Spinal. Disord. Tech.* **2005**, *18*, 58–65. [CrossRef] [PubMed]

6.   Lo, H.J.; Chen, H.M.; Kuo, Y.J.; Yang, S.W. Effect of different designs of interspinous process devices on the instrumented and adjacent levels after double-level lumbar decompression surgery: A finite element analysis. *PLoS ONE* **2020**, *15*, e0244571. [CrossRef] [PubMed]

7.   Shen, H.; Fogel, G.R.; Zhu, J.; Liao, Z.; Liu, W. Biomechanical analysis of different lumbar interspinous process devices: A finite element study. *World Neurosurg.* **2019**, *127*, e1112–e1119. [CrossRef]

8.   Xu, C.; Ni, W.F.; Tian, N.F.; Hu, X.Q.; Li, F.; Xu, H.Z. Complications in degenerative lumbar disease treated with a dynamic interspinous spacer (Coflex). *Int. Orthop.* **2013**, *37*, 2199. [CrossRef] [PubMed]

9.   Toth, J.M.; Bric, J.D. An evaluation of the host response to an interspinous process device based on a series of spine explants: Device for Intervertebral Assisted Motion (DIAM). *J. Spine Surg.* **2019**, *5*, 483–495. [CrossRef] [PubMed]

10.   Li, C.Y.; Chen, M.Y.; Chang, C.N.; Yan, J.L. Three-dimensional volumetric changes and clinical outcomes after decompression with DIAM implantation in patients with degenerative lumbar spine diseases. *Medicine* **2020**, *56*, 723.

11.   Lo, H.J.; Chen, C.S.; Chen, H.M.; Yang, S.W. Application of an interspinous process device after minimally invasive lumbar decompression could lead to stress redistribution at the pars interarticularis: A finite element analysis. *BMC Musculoskelet Disord.* **2019**, *20*, 213. [CrossRef] [PubMed]

12.   Chen, C.S.; Shih, S.L. Biomechanical analysis of a new lumbar interspinous device with optimized topology. *Med. Biol. Eng. Comput.* **2018**, *56*, 1333–1341. [CrossRef] [PubMed]

13.   Guo, L.X.; Yin, J.Y. Finite element analysis and design of an interspinous device using topology optimization. *Med. Biol. Eng. Comput.* **2019**, *57*, 89–98. [CrossRef] [PubMed]

14.   Bae, I.S.; Bak, K.H.; Chun, H.J.; Ryu, J.I.; Park, S.J.; Lee, S.J. Biomechanical analysis of a newly developed interspinous process device conjunction with interbody cage based on a finite element model. *PLoS ONE* **2020**, *15*, e0243771.

15.   Shen, H.; Fogel, G.R.; Zhu, J.; Liao, Z.; Liu, W. Biomechanical analysis of lumbar fusion with proximal interspinous process device implantation. *Int. J. Numer. Method Biomed. Eng.* **2021**, *37*, e3498. [CrossRef] [PubMed]

16.   Zhong, Z.C.; Hung, C.; Lin, H.M.; Wang, Y.H.; Huang, C.H.; Chen, C.S. The influence of different magnitudes and methods of applying preload on fusion and disc replacement constructs in the lumbar spine: A finite element analysis. *Comput. Methods Biomech. Biomed. Eng.* **2013**, *16*, 943–953. [CrossRef]

17.   Rohlmann, A.; Neller, S.; Claes, L.; Bergmann, G.; Wilke, H.J. Influence of a follower load on intradiscal pressure and interseg-mental rotation of the lumbar spine. *Spine* **2001**, *26*, E557–E561. [CrossRef] [PubMed]

18.   Panjabi, M.M. Hybrid multidirectional test method to evaluate spinal adjacent-level effects. *Clin. Biomech.* **2007**, *22*, 257–265. [CrossRef]

19.   Tai, C.L.; Hsieh, P.H.; Chen, W.P.; Chen, L.H.; Chen, W.J.; Lai, P.L. Biomechanical comparison of lumbar spine instability between laminectomy and bilateral laminotomy for spinal stenosis syndrome—An experimental study in porcine model. *BMC Musculoskelet Disord.* **2008**, *9*, 84. [CrossRef] [PubMed]

20.   Zander, T.; Rohlmann, A.; Klöckner, C.; Bergmann, G. Influence of graded facetectomy and laminectomy on spinal biomechanics. *Eur. Spine J.* **2003**, *12*, 427–434. [CrossRef]

21.   Goel, V.K.; Nishiyama, K.; Weinstein, J.; Liu, Y.K. Mechanical properties of lumbar spinal motion segments as affected by partial disc removal. *Spine* **1986**, *11*, 1008–1012. [CrossRef] [PubMed]

22.   Shih, S.L.; Liu, C.L.; Huang, L.Y.; Huang, C.H.; Chen, C.S. Effects of cord pretension and stiffness of the Dynesys system spacer on the biomechanics of spinal decompression- a finite element study. *BMC Musculoskelet Disord.* **2013**, *14*, 191. [CrossRef] [PubMed]

23.   Swanson, K.E.; Lindsey, D.P.; Hsu, K.Y.; Zucherman, J.F.; Yerby, S.A. The effects of an interspinous implant on intervertebral disc pressures. *Spine* **2003**, *28*, 26–32. [CrossRef] [PubMed]

24.   Minns, R.J.; Walsh, W.K. Preliminary design and experimental studies of a novel soft implant for correcting sagittal plane instability in the lumbar spine. *Spine* **1997**, *22*, 1819–1825. [CrossRef]